Asymmetric entanglement for quantum target sensing

Su-Yong Lee,[1,2] Jihwan Kim,[1] Zaeill Kim,[1] and Duk Y. Kim[1]
[1]*Advanced Defense Science and Technology Research Institute, Agency for Defense Development, Daejeon 34186, Korea*
[2]*Weapon Systems Engineering, ADD School, University of Science and Technology, Daejeon 34060, Korea*

(Received 28 February 2024; accepted 16 April 2024; published 30 April 2024)

Entanglement is beneficial to enhancing a phase sensitivity beyond the classical limit that is given by a coherent state. The best performance is achieved with symmetric entangled states, which is enhanced further by sending more photons to the signal mode. We delve into which entanglement structure is valuable for quantum target sensing, such as a reflectivity parameter. We show that an asymmetric entangled state can approach the local joint measurement bound of a two-mode squeezed vacuum state which is a nearly optimal input state for quantum target sensing, whereas it cannot beat the performance of the coherent state for quantum phase sensing. The result is demonstrated with an asymmetric entangled coherent state whose performance is evaluated with quantum Fisher information and confirmed by the signal-to-noise ratio with an optimal observable. The best quantum advantage is achieved in the case of sending fewer photons to the signal mode and many more photons to the idler mode.

DOI: 10.1103/PhysRevA.109.042429

I. INTRODUCTION

Phase sensing arises from gravitational wave detection using the Laser Interferometer Gravitational-Wave Observatory (LIGO) [1], where a beam path-length difference verifies the existence of a gravitational wave. In a laboratory, the beam path-length difference is artificially simulated by putting a phase shifter in one arm of an interferometer. The phase sensitivity is derived by postprocessing the measurement outcomes in the output ports of the interferometer. As a classical benchmark, a coherent-state light is injected into an input port of the interferometer. It is enhanced by adding a squeezed state light into the other input port [2], where the input state is transformed into an entangled state after the first beam splitter. Fundamentally, entanglement can enhance the phase sensitivity by the mean photon number of a signal mode (N_S), assuming the phase sensitivity is represented by a mean-squared error. The fundamental scaling limit is achieved by the combination of a coherent state and squeezed vacuum state [2], a single-mode squeezed state [3,4], a two-mode squeezed vacuum (TMSV) state [5], NOON-type states [1,6–9], and other types of entangled states [10,11].

Aside from the phase parameter, there is another interesting parameter, such as reflectivity (or transmittivity) of a target that determines the detection intensity in a receiver. In a thermal-noise environment, the scenario of sensing the target reflectivity is related to quantum illumination [12,13] that discriminates the presence or absence of a target with entangled states in a strong thermal-noise environment. The target sensitivity can be lower bounded by an inverse of quantum Fisher information (QFI) and the target discrimination is evaluated by detection error probability. Assuming the target reflectivity (η) is close to zero, the associated QFI at $\eta = 0$ provides information on an upper bound of the minimum detection error probability with a local joint measurement [14], which is given by $P_{\rm err} \leqslant \frac{1}{2}\exp[-\frac{\eta^2 M H(\rho_0)}{8}]$. H represents the QFI at $\eta = 0$ and M is the number of modes. In case of the QFI at $\eta = 0$, there is no difference between a passive signature and no passive signature by thermal noise [15–20], where the passive signature represents the probability of detecting a target without sending any signal. The larger is the QFI, the smaller is the detection error probability. There have been a few studies between quantum target sensing and quantum illumination [18,21–25]. It is known that the TMSV state is a nearly optimal entangled state [26–28] for quantum illumination and it also presents the best performance in quantum target sensing [14] even if cat states can approach the performance of the TMSV state at a low signal mean photon number.

Here, we show that two-mode asymmetric entangled states can take quantum advantage over the classical bound for quantum target sensing, in particular, when fewer photons are sent to the signal mode and more photons are sent to the idler mode. In general, an arbitrary two-mode asymmetric entangled state can be represented by $|f_1\rangle_S|g_1\rangle_I + |f_2\rangle_S|g_2\rangle_I$, where $|f_{1(2)}\rangle$ and $|g_{1(2)}\rangle$ are arbitrary single-mode states with $\langle f_2|f_1\rangle \neq 0$ and $\langle g_2|g_1\rangle \neq 0$. In order to control the mean photon number ratio between the signal and idler modes, in continuous variable systems, one of the best candidates is a coherent state rather than squeezed states. Using coherent states, we consider an asymmetric entangled coherent state (AECS) $(|\alpha\rangle_S|\beta\rangle_I + |-\alpha\rangle_S|-\beta\rangle_I)$ for quantum target sensing. The entangled coherent state is produced by injecting an even-cat state $(|\alpha_1\rangle_S + |-\alpha_1\rangle_S)$ into a beam splitter, where the mean photon number ratio between the signal and idler modes is controlled by the beam-splitting ratio (t, r) under this relation of $\alpha \equiv t\alpha_1$, $\beta \equiv r\alpha_1$, and $t^2 + r^2 = 1$, as shown in Fig. 1. We present that the AECS is not beneficial for quantum phase sensing but for quantum target sensing.

This paper is organized as follows. We introduce QFI for quantum parameter sensing, especially for the phase parameters. The QFI is applied to quantum target sensing that pays attention to target reflectivity using symmetric and

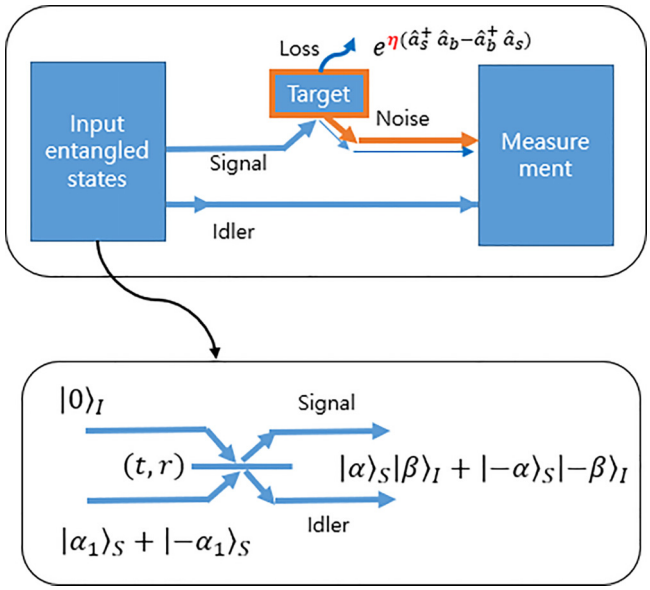

FIG. 1. Schematic of quantum target sensing (upper panel), where the thermal-noise environment is displayed with a thick orange line. Generation of an asymmetric entangled coherent state with an even-cat state and a beam splitter having $t^2 + r^2 = 1$, $\alpha = t\alpha_1$ and $\beta = r\alpha_1$ (lower panel).

asymmetric entangled states. In particular, an AECS is analytically investigated with its optimal observable, even in some ranges of signal and idler mean photon numbers. Then, we conclude with a summary and discussion.

II. QUANTUM FISHER INFORMATION

Fisher information (FI) represents a quantitative measure of the small change of a parameter with a specific measurement setup. The small change of a parameter is represented by the variance, demonstrating a parameter sensitivity. Under an optimal positive operator-valued measure, FI is maximized as quantum Fisher information (QFI). For an unbiased estimator where a mean value of an estimator is equal to the true value of a parameter, the lower bound of the parameter sensitivity is proportional to the inverse of the QFI, $\Delta^2 X \geqslant 1/[mH(X)]$, where m is the number of trials and H is the QFI. The larger is the QFI, the more enhanced is the parameter sensitivity.

For quantum phase sensing, the phase sensitivity is tested in an interferometer, where a phase shifter is located on one arm. Using a generator (i.e., a number operator) of the phase shifter, it is obtained that the QFI of the standard quantum state (i.e., coherent state) is upper bounded by a signal mean photon number (N_S). The associated QFI can be increased by using a single-mode squeezed vacuum state [2,3] and path-symmetric entangled states [29] that attain the fundamental quantum limit of the phase sensitivity. The nonclassical states enhance the phase sensitivity by as many as N_S. The path-symmetric entangled states include a TMSV state [5] and NOON-type entangled states [7,8]. In a lossy interferometer, path-symmetric entangled states are still beneficial for quantum enhancement but a concrete shape of entanglement is changed depending on a loss model [30,31]. For example, it is the best strategy for preparing a symmetric entangled coherent state $(|\alpha\rangle_S|\beta\rangle_I + |\beta\rangle_S|\alpha\rangle_I)$ with a smaller mean photon number difference between the signal and idler modes under increasing loss, where more photons on both input modes can survive even after severe loss.

Instead of symmetric entangled states, we may also consider asymmetric entangled states for quantum phase sensing. For example, it is investigated with an AECS $(|\alpha\rangle_S|\beta\rangle_I + |-\alpha\rangle_S|-\beta\rangle_I)$. Regardless of choosing α and β, the associated QFI is upper bounded by N_S whose inverse demonstrates the coherent-state limit. Thus, an asymmetric entangled state cannot beat the performance of the coherent state for phase sensitivity, resulting in no quantum enhancement. However, we show that the asymmetric entangled state can take a quantum advantage for quantum target sensing in the next section.

III. QUANTUM TARGET SENSING

Target sensing is physically simulated with a beam splitter whose reflectivity $[\eta = \sin(\theta/2)]$ is to estimate. In the limit of $\theta \ll 1$, the beam-splitting operation is approximated as $\exp[\eta(\hat{a}_s^\dagger \hat{a}_b - \hat{a}_b^\dagger \hat{a}_s)]$, where the subscript s represents a signal mode and b represents a thermal-noise mode. In Fig. 1, a signal mode is reflected from a target having a reflectivity (η) and then the reflected mode including thermal noise is measured with an idler mode in a receiver. The target sensitivity is inversely proportional to QFI at $\eta = 0$ since we are interested in a small change at $\eta = 0$.

With no thermal noise, the QFI becomes $4N_S$ regardless of the coherent state, TMSV state, and other entangled states. With thermal noise, the TMSV state takes quantum advantage over the coherent state [14], irrespective of N_S. The amount of quantum advantage increases with sending fewer photons to the signal mode. Since the mean photon number of the idler mode is the same as that of the signal mode, it is the best strategy for sending fewer signal mean photon numbers of the TMSV state to a target. As another type of symmetric entangled state, we consider a symmetric entangled coherent state (SECS) $(|\alpha\rangle_S|\beta\rangle_I + |\beta\rangle_S|\alpha\rangle_I)$. Although it approaches the coherent-state bound when $\beta = -\alpha$ and $|\alpha|^2 \gg 1$, the SECS cannot take a quantum advantage over the coherent state.

A. Asymmetric entangled coherent state

We consider an asymmetric entangled coherent state (AECS) as a test function of an asymmetric entangled state. Mathematically, the AECS is represented by a nonorthogonal coherent-state basis that can be transformed into orthogonal even- and odd-cat state bases,

$$\begin{aligned}|\mathrm{AECS}\rangle &\equiv \frac{1}{\sqrt{M}}(|\alpha\rangle_S|\beta\rangle_I + |-\alpha\rangle_S|-\beta\rangle_I) \\ &= \frac{1}{\sqrt{2M}}\left(\sqrt{N_o^\alpha N_o^\beta}|o_\alpha\rangle_S|o_\beta\rangle_I + \sqrt{N_e^\alpha N_e^\beta}|e_\alpha\rangle_S|e_\beta\rangle_I\right),\end{aligned} \tag{1}$$

where $N_o^A = 2(1 - e^{-2|A|^2})$, $N_e^A = 2(1 + e^{-2|A|^2})$, $M = 2(1 + e^{-2(|\alpha|^2+|\beta|^2)})$, $|o_A\rangle = (|A\rangle - |-A\rangle)/\sqrt{N_o^A}$, and $|e_A\rangle = (|A\rangle + |-A\rangle)/\sqrt{N_e^A}$ $(A = \alpha, \beta)$. $|e_A\rangle$ and $|o_A\rangle$ are the even- and odd-cat state bases, respectively. The mean photon numbers of

the signal and idler modes are given by $N_S = \frac{|\alpha|^2(1-e^{-2(|\alpha|^2+|\beta|^2)})}{(1+e^{-2(|\alpha|^2+|\beta|^2)})}$ and $N_I = \frac{|\beta|^2(1-e^{-2(|\alpha|^2+|\beta|^2)})}{(1+e^{-2(|\alpha|^2+|\beta|^2)})}$, respectively. N_S increases with an increase in $|\alpha|$, and it is the same as the relation between N_I and $|\beta|$.

Since it is a pure bipartite state, we derive the degree of entanglement (DOE) by using the von Neumann entropy, as shown below,

$$\mathrm{DOE} = -\sum_{k=o,e} \frac{N_k^\alpha N_k^\beta}{4M} \log_2 \frac{N_k^\alpha N_k^\beta}{4M}. \tag{2}$$

The DOE increases by increasing α or β or both α and β. From the QFI of Eq. (1), we figure out that the amount of entanglement does not guarantee a quantum advantage for quantum target sensing.

Using a formula of Ref. [14], the QFI of the AECS is derived as

$$H_{\eta=0} = \frac{|\alpha|^2 N_o^\beta N_e^\beta}{M(1+N_B)}\left[\frac{\left(N_e^\alpha\right)^2}{N_e^\alpha N_e^\beta + N_o^\alpha N_o^\beta \frac{N_B}{1+N_B}} + \frac{\left(N_o^\alpha\right)^2}{N_o^\alpha N_o^\beta + N_e^\alpha N_e^\beta \frac{N_B}{1+N_B}}\right]. \tag{3}$$

In the limit of $N_S \ll 1 \ll N_I$, the QFI approaches $4N_S/(1+N_B)$ that is the same as the QFI of the TMSV state. N_B is the mean photon number of thermal noise. In that regime, we compare the performance of the AECS with the TMSV state and coherent state, as shown in Fig. 2. We obtain that the AECS approaches the performance of the TMSV state when having a smaller signal mean photon number under a high idler mean photon number, resulting in a larger quantum advantage over the coherent state.

Assuming α is real valued, we obtain the corresponding symmetric logarithmic derivative (SLD) as

$$\hat{L} = \frac{(-\sqrt{2})}{1+N_B}[(c_1+c_2)(|o_\beta\rangle_I\langle e_\beta| + |e_\beta\rangle_I\langle o_\beta|)\otimes \hat{X}_b + i(c_1-c_2)(|o_\beta\rangle_I\langle e_\beta| - |e_\beta\rangle_I\langle o_\beta|)\otimes \hat{P}_b], \tag{4}$$

where $\hat{X}_b = (\hat{b}+\hat{b}^\dagger)/\sqrt{2}$, $\hat{P}_b = (\hat{b}-\hat{b}^\dagger)/i\sqrt{2}$, $c_1 = \frac{\alpha\sqrt{N_o^\beta N_e^\beta}}{2\sqrt{M}} \frac{N_o^\alpha}{\sqrt{N_o^\alpha N_o^\beta}+\sqrt{N_e^\alpha N_e^\beta}\frac{N_B}{1+N_B}}$, and $c_2 = \frac{\alpha\sqrt{N_o^\beta N_e^\beta}}{2\sqrt{M}} \frac{N_e^\alpha}{\sqrt{N_e^\alpha N_e^\beta}+\sqrt{N_o^\alpha N_o^\beta}\frac{N_B}{1+N_B}}$. The SLD consists of correlated measurement operators. The eigenbasis of the SLD presents the optimal measurement basis [32], but the measurement basis cannot be simply constructed due to the noncommutativity of each component observable of Eq. (4).

In the limit of $N_S \ll 1 \ll N_I$, the SLD is simplified as

$$\hat{L} \approx \frac{-\sqrt{2}c_2}{(1+N_B)}\left(|o_\beta\rangle_I\langle e_\beta|\otimes\hat{b}^\dagger + |e_\beta\rangle_I\langle o_\beta|\otimes\hat{b}\right), \tag{5}$$

and the AECS is approximated as

$$|\mathrm{AECS}\rangle \approx \frac{1}{\sqrt{1+|\alpha|^2}}(|0\rangle_S|e_\beta\rangle_I + \alpha|1\rangle_S|o_\beta\rangle_I). \tag{6}$$

The corresponding optimal observable is defined as $\hat{O} \equiv \hat{L}\frac{(1+N_B)}{(-\sqrt{2}c_2)}$ that is transformed by a reverse target interaction

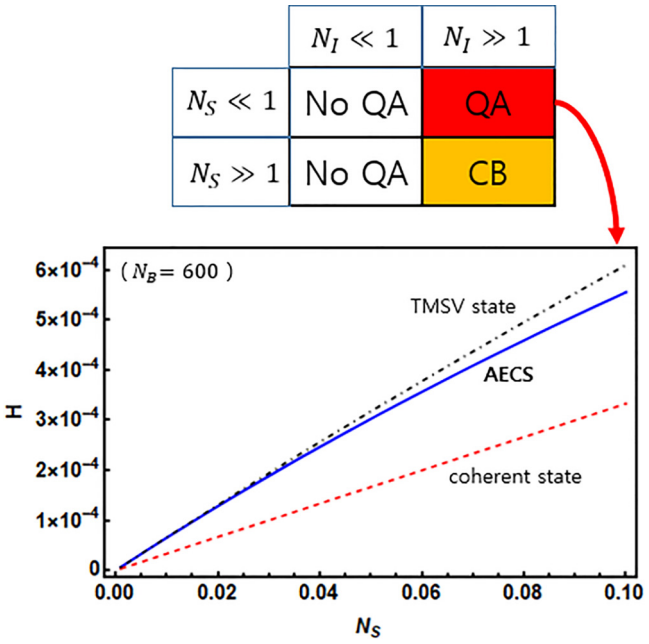

FIG. 2. Quantum advantage (QA) region for an asymmetric entangled coherent state. CB presents the classical bound with a coherent state. N_S (N_I) is the signal (idler) mean photon number. Quantum Fisher information as a function of signal mean photon number for quantum reflectivity sensing (lower panel), where the blue solid curve represents an asymmetric entangled coherent state (AECS) with $N_I = 10$. N_B is the mean photon number of thermal noise.

as follows,

$$\hat{O}_\eta = |o_\beta\rangle_I\langle e_\beta|\otimes(\eta\hat{a}_s^\dagger + \sqrt{1-\eta^2}\hat{b}^\dagger) + |e_\beta\rangle_I\langle o_\beta|\otimes(\eta\hat{a}_s + \sqrt{1-\eta^2}\hat{b}). \tag{7}$$

By applying Eq. (7) to Eq. (6) and thermal noise, we obtain its mean and variance, leading to the signal-to-noise ratio (SNR) $\frac{\eta^2 N_S}{2(N_B+1)}$, which approximately corresponds to the local joint measurement bound for the TMSV state. Note that the SNR is defined as $(\langle\hat{O}\rangle_\eta - \langle\hat{O}\rangle_{\eta=0})^2/2(\sqrt{\Delta^2 O_\eta} + \sqrt{\Delta^2 O_{\eta=0}})^2$ [16,33], which is an exponent of the detection error probability as $P_{\mathrm{err}} = \frac{1}{2}\exp(-M\times\mathrm{SNR})$. From the viewpoint of the detection error probability $P_{\mathrm{err}} = \frac{1}{2}\exp(-\frac{\eta^2 MH}{8})$, it is the same as the result of the QFI of Eq. (3).

B. Approximated form in the other range of N_S, N_I

In Fig. 2, except for the limit of $N_S \ll 1 \ll N_I$, we find that there is no quantum advantage. A large signal mean photon number does not guarantee a quantum advantage over the coherent-state bound, which is understood by its approximated form of Eq. (1).

First, for $N_I \ll 1 \ll N_S$, the AECS is approximated as

$$|\mathrm{AECS}\rangle \approx \frac{1}{\sqrt{1+|\beta|^2}}(|e_\alpha\rangle_S|0\rangle_I + \beta|o_\alpha\rangle_S|1\rangle_I). \tag{8}$$

Since the idler mean photon number (N_I) is much smaller than one, the associated QFI is approximated as $8N_S N_I/N_B$ with its optimal observable $\hat{O} = (|1\rangle_I\langle 0| + |0\rangle_I\langle 1|)\otimes\hat{X}_b$, which is

worse than the coherent-state bound, $4N_S/(1+2N_B)$. Under $N_I \ll 1$, increasing the signal mean photon number provides a negative performance in target sensing since we lose more photons in the signal mode.

Second, for $1 \ll N_S, N_I$, the AECS is approximated as

$$|\text{AECS}\rangle \approx \tfrac{1}{\sqrt{2}}(|o_\alpha\rangle_S|o_\beta\rangle_I + |e_\alpha\rangle_S|e_\beta\rangle_I). \tag{9}$$

It is the same as the maximal two-qubit entangled state such that the associated QFI approaches $4N_S/(1+2N_B)$ with its optimal observable $\hat{O} = (|o_\beta\rangle_I\langle e_\beta| + |e_\beta\rangle_I\langle o_\beta|) \otimes \hat{X}_b$, corresponding to the coherent-state bound. When both mean photon numbers of the signal and the idler modes increase, increasing the idler mean photon number compensates the negative effect produced by increasing the signal mean photon number, but its performance cannot overcome the coherent-state bound.

Third, for $N_S, N_I \ll 1$, the AECS is approximated as

$$|\text{AECS}\rangle \approx \frac{1}{\sqrt{1+|\alpha\beta|^2}}(|0\rangle_S|0\rangle_I + \alpha\beta|1\rangle_S|1\rangle_I). \tag{10}$$

Surprisingly, it is the same as an approximated form of the TMSV state so that Eq. (10) provides a quantum advantage over the classical bound, where the optimal observable is given by $\hat{O} = |0\rangle_I\langle 1| \otimes \hat{b} + |1\rangle_I\langle 0| \otimes \hat{b}^\dagger$. However, it contradicts the result of Fig. 2, due to each coherent state being approximated as $|\alpha\rangle \approx |0\rangle + \alpha|1\rangle$, where the coherent state is a classical state but its approximated form represents a nonclassical state. We emphasize that the approximation in the range is not valid for the interpretation of the result of Fig. 2, due to oversimplification.

C. Relative phase effect of the AECS

We may ask what occurs if we change the relative phase of the AECS. Putting a minus sign between the two parts in the input state of Eq. (1), we obtain a transformed AECS as follows,

$$\begin{aligned}|\text{AECS}_{(-)}\rangle &\equiv \frac{1}{\sqrt{M_{(-)}}}(|\alpha\rangle_S|\beta\rangle_I - |-\alpha\rangle_S|-\beta\rangle_I) \\ &= \frac{1}{\sqrt{2M_{(-)}}}\Big(\sqrt{N_o^\alpha N_e^\beta}|o_\alpha\rangle_S|e_\beta\rangle_I \\ &\quad + \sqrt{N_e^\alpha N_o^\beta}|e_\alpha\rangle_S|o_\beta\rangle_I\Big),\end{aligned} \tag{11}$$

where the normalization constant changes the sign as $M_{(-)} = 2(1-e^{-2(|\alpha|^2+|\beta|^2)})$. There is an exchange between the even- and odd-cat state bases in the idler mode ($|e_\beta\rangle_I$ and $|o_\beta\rangle_I$), along with the exchange of β components (N_e^β and N_o^β). The mean photon number of the signal mode is given by $N_S^{(-)} = \frac{|\alpha|^2(1+e^{-2(|\alpha|^2+|\beta|^2)})}{(1-e^{-2(|\alpha|^2+|\beta|^2)})}$.

The associated QFI is derived with an exchange of β components in the idler mode,

$$\begin{aligned}H_{\eta=0}^{(-)} = \frac{|\alpha|^2 N_o^\beta N_e^\beta}{M(1+N_B)}\Bigg[&\frac{(N_e^\alpha)^2}{N_e^\alpha N_o^\beta + N_o^\alpha N_e^\beta \frac{N_B}{1+N_B}} \\ &+ \frac{(N_o^\alpha)^2}{N_o^\alpha N_e^\beta + N_e^\alpha N_o^\beta \frac{N_B}{1+N_B}}\Bigg].\end{aligned} \tag{12}$$

There is no change in the results of Figs. 1 and 2. Except for $N_S, N_I \ll 1$, there exists only a basis exchange in the approximated forms for other ranges of N_S and N_I. For $N_S \ll 1 \ll N_I$, the transformed AECS is approximated as

$$|\text{AECS}_{(-)}\rangle \approx \frac{(|0\rangle_S|o_\beta\rangle_I + \alpha|1\rangle_S|e_\beta\rangle_I)}{\sqrt{1+|\alpha|^2}}, \tag{13}$$

where the idler-mode basis has exchanged compared to Eq. (6). For $N_I \ll 1 \ll N_S$, it is approximated as

$$|\text{AECS}_{(-)}\rangle \approx \frac{(|o_\alpha\rangle_S|0\rangle_I + \beta|e_\alpha\rangle_S|1\rangle_I)}{\sqrt{1+|\beta|^2}}, \tag{14}$$

where the signal-mode basis has exchanged compared to Eq. (8). For $1 \ll N_S, N_I$, it is approximated as

$$|\text{AECS}_{(-)}\rangle \approx \frac{(|o_\alpha\rangle_S|e_\beta\rangle_I + |e_\alpha\rangle_S|o_\beta\rangle_I)}{\sqrt{2}}, \tag{15}$$

where the idler-mode basis has exchanged compared to Eq. (9). For each case, the corresponding optimal observable is also derived from the corresponding SLD. We skip this process because it does not change the results of this section.

For $N_S, N_I \ll 1$, it is approximated as

$$|\text{AECS}_{(-)}\rangle \approx \frac{(\alpha|1\rangle_S|0\rangle_I + \beta|0\rangle_S|1\rangle_I)}{\sqrt{|\alpha|^2+|\beta|^2}}, \tag{16}$$

which provides a different interpretation of Eq. (10) that contradicts the result in Fig. 2. Assuming $\alpha = \beta$, the transformed AECS of Eq. (16) is a maximal single-photon entangled state that approaches the coherent-state bound. That does not explain the result of Fig. 2, due to oversimplification of the coherent state, either.

IV. SUMMARY AND DISCUSSION

We present an asymmetric entangled state that can approach the local joint measurement bound of a TMSV state for quantum target sensing, when the signal mean photon number (N_S) is much smaller than one and the idler mean photon number (N_I) is much larger than one. Using an AECS, specifically, we showed a quantum advantage by its QFI according to the range of signal and idler mean photon numbers. It was also confirmed by its SNR with an optimal observable in the limit of $N_S \ll 1 \ll N_I$. The result is maintained even with a change of the relative phase of the AECS.

It is natural to contemplate how to construct the optimal observable that approaches the local joint measurement bound for the TMSV state. Previously, it was briefly mentioned in Ref. [14] that this requires the Jaynes-Cummings model. Here, we provide a concrete example. Looking into the observable $\hat{O} = |o_\beta\rangle_I\langle e_\beta| \otimes \hat{b}^\dagger + |e_\beta\rangle_I\langle o_\beta| \otimes \hat{b}$ that is related to Eq. (7), the receiver should consist of a two-level system in the idler mode and a cavity system in the reflected mode, where the two-level system interacts with the cavity field. If the two-level system consists of an even-cat state (excited state) and an odd-cat state (ground state), then the operator $\hat{b}^\dagger$ or $\hat{b}$ is applied to the cavity field by interacting with the two-level system. However, due to the noncommutativity of the each component of the observable, it is not possible to find the eigenbasis of the observable $\hat{O}$ in the idler and reflected

modes. This issue also occurred in the local joint measurement bound for the TMSV state, where the optimal observable $\hat{X}_S\hat{X}_I - \hat{P}_S\hat{P}_I$ cannot be exactly implemented [17] but it can be closely implemented with a phase conjugate or optical parametric amplifier receiver [33] at a low signal mean photon number. Thus, in the near future, we are interested in finding a receiver close to the local joint measurement bound for the AECS.

It is intriguing that the fewer number of photons in a signal mode of the AECS (or TMSV state) can enhance the quantum advantage over a coherent state. Here, the quantum advantage is represented by (QFI of the AECS)/(QFI of the coherent state). Actually, increasing the number of photons in the signal mode increases the amount of the QFI of the AECS but decreases the quantum advantage over the coherent state. It is understood that a smaller signal mean photon number provides a larger quantum entanglement effect in quantum target sensing. We expect that this idea could be applied to any asymmetric interferometric configurations in quantum sensing.

ACKNOWLEDGMENTS

This work was supported by a grant to Defense-Specialized Project funded by Defense Acquisition Program Administration and Agency for Defense Development.

[1] J. P. Dowling, Contemp. Phys. **49**, 125 (2008).
[2] C. M. Caves, Phys. Rev. D **23**, 1693 (1981).
[3] A. Monras, Phys. Rev. A **73**, 033821 (2006).
[4] C. Oh, C. Lee, C. Rockstuhl, H. Jeong, J. Kim, H. Nha, and S.-Y. Lee, npj Quantum Inf. **5**, 10 (2019).
[5] P. M. Anisimov, G. M. Raterman, A. Chiruvelli, W. N. Plick, S. D. Huver, H. Lee, and J. P. Dowling, Phys. Rev. Lett. **104**, 103602 (2010).
[6] J. Joo, W. J. Munro, and T. P. Spiller, Phys. Rev. Lett. **107**, 083601 (2011).
[7] S.-Y. Lee, C.-W. Lee, H. Nha, and D. Kaszlikowski, J. Opt. Soc. Am. B **32**, 1186 (2015).
[8] S.-Y. Lee, C.-W. Lee, J. Lee, and H. Nha, Sci. Rep. **6**, 30306 (2016).
[9] S.-W. Lee, S.-Y. Lee, and J. Kim, J. Opt. Soc. Am. B **37**, 2423 (2020).
[10] M. J. Holland and K. Burnett, Phys. Rev. Lett. **71**, 1355 (1993).
[11] S. D. Huver, C. F. Wildfeuer, and J. P. Dowling, Phys. Rev. A **78**, 063828 (2008).
[12] S. Lloyd, Science **321**, 1463 (2008).
[13] S. H. Tan, B. I. Erkmen, V. Giovannetti, S. Guha, S. Lloyd, L. Maccone, S. Pirandola, and J. H. Shapiro, Phys. Rev. Lett. **101**, 253601 (2008).
[14] M. Sanz, U. Las Heras, J. J. García-Ripoll, E. Solano, and R. Di Candia, Phys. Rev. Lett. **118**, 070803 (2017).
[15] S. Pirandola, B. R. Bardhan, T. Gehring, C. Weedbrook, and S. Lloyd, Nat. Photonics **12**, 724 (2018).
[16] Y. Jo, S. Lee, Y. S. Ihn, Z. Kim, and S.-Y. Lee, Phys. Rev. Res. **3**, 013006 (2021).
[17] S.-Y. Lee, Y. Jo, T. Jeong, J. Kim, D. H. Kim, D. Kim, D. Y. Kim, Y. S. Ihn, and Z. Kim, Phys. Rev. A **105**, 042412 (2022).
[18] R. Jonsson and R. Di Candia, J. Phys. A: Math. Theor. **55**, 385301 (2022).
[19] T. J. Volkoff, J. Phys. A: Math. Theor. **57**, 065301 (2024).
[20] G. Y. Tham, R. Nair, and M. Gu, arXiv:2310.11013.
[21] S.-Y. Lee, Y. S. Ihn, and Z. Kim, Phys. Rev. A **103**, 012411 (2021).
[22] C. Noh, C. Lee, and S.-Y. Lee, J. Opt. Soc. Am. B **39**, 1316 (2022).
[23] Z. Gong, N. Rodriguez, C. N. Gagatsos, S. Guha, and B. A. Bash, IEEE J. Sel. Top. Signal Process. **17**, 473 (2023).
[24] M. Casariego, Y. Omar, and M. Sanz, Adv. Quantum Technol. **5**, 2100051 (2022).
[25] W. Zhong, W.-Y. Zhu, Y. Li, L. Zho, M.-M. Du, and Y.-B. Sheng, arXiv:2308.07150.
[26] R. Nair and M. Gu, Optica **7**, 771 (2020).
[27] M. Bradshaw, L. O. Conlon, S. Tserkis, M. Gu, P. K. Lam, and S. M. Assad, Phys. Rev. A **103**, 062413 (2021).
[28] G. De Palma and J. Borregaard, Phys. Rev. A **98**, 012101 (2018).
[29] H. F. Hofmann, Phys. Rev. A **79**, 033822 (2009).
[30] R. Demkowicz-Dobrzanski, U. Dorner, B. J. Smith, J. S. Lundeen, W. Wasilewski, K. Banaszek, and I. A. Walmsley, Phys. Rev. A **80**, 013825 (2009).
[31] S.-Y. Lee, Y. S. Ihn, and Z. Kim, Phys. Rev. A **101**, 012332 (2020).
[32] M. G. A. Paris, Int. J. Quantum Inf. **07**, 125 (2009).
[33] S. Guha and B. I. Erkmen, Phys. Rev. A **80**, 052310 (2009).